Research on Engineering Structures & Materials
www.jresm.org
MIM Research Group

Research Article

Height-dependent seismic performance of reinforced concrete buildings in Portoviejo: A comparative study on the influence of masonry infill walls and staircases

María Belén Mera [a], Brian Cagua Gómez [*,b]

Master's Program in Civil Engineering, specialization in Structures, Universidad Técnica de Manabí, Portoviejo, Ecuador

Article Info

Article History:

Received 26 Jun 2026

Accepted 01 Oct 2026

Keywords:

Masonry infill walls;
Staircases;
Pushover analysis;
Soft-story mechanism;
Capacity curves;
Ecuador

Abstract

The seismic response of reinforced concrete buildings can be significantly affected by masonry infill walls and staircases, which are often not explicitly considered in analytical models. This study evaluates the effect of these components on typical buildings in Portoviejo, Ecuador, to identify their influence on structural capacity and seismic performance. Three representative building typologies of 3, 6, and 10 stories were analyzed through nonlinear static pushover analysis, performed in SeismoStruct using inelastic force-based frame elements with fiber sections, considering four structural configurations: frame (P), frame with masonry infill walls (P+M), frame with staircases (P+S), and frame with masonry infill walls and staircases (P+M+S). Based on the capacity curves, performance points, and damage distribution, the results indicate that the influence of these components depends on building height. In low-rise buildings, masonry infill walls increased the initial stiffness by approximately 90–110% and the lateral strength relative to the bare frame, although they reduced global ductility. In mid-rise buildings, the most critical response was observed, associated with vertical irregularity, damage concentration in the lower stories, and a tendency toward soft-story mechanisms, consistent with field observations following the 2016 Portoviejo earthquake. In high-rise buildings, the global effect was smaller, although local effects on the distribution of internal forces and damage remained. These findings indicate that neglecting masonry infill walls and staircases may underestimate relevant seismic demands and misrepresent stiffness, deformation patterns, and damage concentration; therefore, their explicit consideration is recommended in the seismic assessment of existing reinforced concrete buildings with similar configurations in Portoviejo.

© 2026 MIM Research Group. All rights reserved.

1. Introduction

Performance-based seismic assessment of buildings has become particularly relevant in regions of high seismic hazard, as it allows not only the structural safety against severe seismic events to be estimated, but also the expected deformation, damage level, and post-earthquake functionality at different levels of seismic demand. For the existing building stock, this framework is a necessary basis for assessment rather than a general analytical tool, because structural safety depends on the capacity to sustain inelastic deformations and on how damage concentrates as seismic demand increases [1-3]. In framed buildings, this assessment is especially important for irregular reinforced concrete (RC) buildings, where nonuniform distributions of stiffness and strength may concentrate inelastic demands in specific stories or structural members.

*Corresponding author: brian.cagua@utm.edu.ec
[a]orcid.org/0009-0002-6240-664X; [b]orcid.org/0000-0003-2530-8549
DOI: http://dx.doi.org/10.17515/resm2026-1797st0626rs

In the Ecuadorian context, and particularly in Portoviejo, this issue is especially relevant because the city is located in a zone of high seismic hazard [4,5]. The damage observed during the April 16, 2016 earthquake, revealed the vulnerability of a significant portion of the reinforced concrete building stock, particularly in buildings with open ground stories, irregularities in story height, and a substantial reduction of masonry infill walls at the first level [6,7]. Approximately 40 RC buildings collapsed in downtown Portoviejo, with contributing factors that included seismic demands exceeding the code spectra at periods of about 0.5 s, the addition of stories without structural strengthening, highly flexible structural systems, and typologies with tall ground stories and mezzanines [7]. Field observations and three-dimensional pushover analysis of a representative RC building further highlighted the significant influence of masonry infill walls on the observed seismic response [8]. The combination of a taller ground story and a reduced density of masonry infill walls at this level can generate a pronounced vertical stiffness irregularity, favoring deformation concentration in the first story and the development of soft-story mechanisms [6, 7, 9]. Numerical analyses of corner buildings that collapsed in Portoviejo have further shown that irregular distributions of masonry infill walls in plan can induce a predominantly torsional response that significantly influences the collapse response [10]. These observations indicate that the seismic response of the local building stock cannot be interpreted exclusively from the properties of the bare RC frame.

Masonry infill walls and staircases are among the components that can significantly modify the response of RC frames, although they are commonly omitted from the explicit representation of the main lateral-load-resisting system. In the case of masonry infill walls, their interaction with the frame may increase the initial stiffness and strength of the system, but may also reduce its ductility and induce more brittle responses and damage concentrations in columns and joints [11-14]. Staircases can likewise modify lateral stiffness, internal-force distribution, and the lateral load path because stair flights and landings provide additional connections between adjacent stories [15-17]. When intermediate landings are connected to frame columns, the effective deformable length of these members may be reduced, increasing local shear demand and promoting a short-column-type response [17]. Recent field observations following the 2023 Kahramanmaraş earthquakes have also documented significant staircase damage, including cracking, shear-related failures, and local collapse, emphasizing the importance of explicitly considering staircase–frame interaction and connection detailing in seismic assessment [18]. Consequently, neglecting staircases in numerical models may conceal both changes in the global structural response and local damage mechanisms in members adjacent to the staircase [17].

A previous study by Ortega and Cagua [19] examined the combined influence of masonry infill walls and staircases on representative low-, mid-, and high-rise RC building typologies in Portoviejo. That study focused on changes in dynamic properties, including vibration periods and modes, and identified potential adverse effects such as short-column behavior, increased base shear, stress redistribution, and soft-story response. It also showed that the relative influence of these components decreases with building height and recommended nonlinear modeling for a more detailed assessment of seismic vulnerability. The present study addresses this need by extending the assessment of these typologies into the nonlinear range. Specifically, four configurations, namely bare frame (P), frame with staircases (P+S), frame with masonry infill walls (P+M), and frame with both components (P+M+S), are compared in terms of capacity curves, performance points for seismic demands associated with return periods of 475 and 2475 years, interstory drift profiles, and the localization and severity of damage in RC members and masonry infill panels.

In this context, the objective of this study is to comparatively evaluate how masonry infill walls and staircases modify the capacity and seismic performance of representative 3-, 6-, and 10-story RC framed buildings in Portoviejo through nonlinear static analysis. By characterizing the variation of global capacity, interstory drift, and local damage distribution among building-height typologies, the study seeks to support more informed assessment and strengthening decisions for existing buildings with similar configurations. The findings also provide technical evidence that may contribute to future refinements of local modeling and seismic-assessment practices within the NEC-SE-DS framework [5], particularly regarding components that modify the lateral response but are frequently omitted from conventional analytical models.

2. Material and Method

2.1 Structural Typologies Analyzed

The study considered three reinforced concrete framed-building typologies representative of the building stock in Portoviejo, Ecuador, corresponding to low-, mid-, and high-rise categories with 3, 6, and 10 stories, respectively. These typologies were defined based on recurring geometric, architectural, and structural characteristics documented through post-earthquake field observations and previous studies of buildings in Portoviejo following the April 16, 2016 earthquake [7,19].

The three typologies reproduce a common architectural layout in the city: a taller ground story with a lower density of masonry infill walls, generally associated with commercial use, and upper stories with a greater density of masonry infill panels associated with residential use. This condition generates a vertical discontinuity in stiffness and strength that may favor the development of soft-story mechanisms and the concentration of deformations at the first level [5], [7]. Uniform spans of l_n = 4.0 m were adopted in both principal directions as a controlled geometric assumption to reduce the number of variables in the comparative analysis, allowing the influence of masonry infill walls and staircases to be evaluated under consistent plan geometry. Consequently, plan irregularities, variable spans, and their associated torsional effects are not represented by the adopted archetypes and are outside the scope of the present comparative assessment. The ground-story height was h_1 = 3.60 m, whereas the upper stories had a constant height of h_n = 3.00 m. The staircase layout was established based on common construction configurations: in the low- and mid-rise buildings, the staircases were located near the interior façade, whereas in the high-rise typology they were placed closer to the structural core. The general plan configuration, masonry infill distribution, staircase location, and three-dimensional representation of each typology are shown in Fig. 1.

The main geometric, material, and reinforcement properties of the three structural typologies are summarized in Tables 1 and 2. Table 1 presents the building height, concrete compressive strength, column dimensions (b_c and h_c), and longitudinal reinforcement (A_s), whereas Table 2 presents the beam dimensions (b_b and h_b) and longitudinal reinforcement adopted for the corresponding story groups.

Table 1. Geometric, material, and column properties of the analyzed structural typologies

Typology	Height (m)	$f'c$ (MPa)	Columns			
			b_c (m)	h_c (m)	Longitudinal reinforcement (A_s)	
Low-rise	9.60	21	0.40	0.40	8 ϕ16 mm	
Mid-rise	18.60	24	0.60	0.60	12 ϕ20 mm	
High-rise	30.60	28	0.80	0.80	Corners	4 ϕ22 mm
					Remaining bars	16 ϕ20 mm

Table 2. Beam dimensions and longitudinal reinforcement of the analyzed structural typologies

Typology	b_b (m)	h_b (m)		Beams	
				Lower-story group	Upper-story group
Low-rise	0.30	0.40	Top	4 ϕ14 mm	-
			Bottom	3 ϕ14 mm	-
Mid-rise	0.35	0.45	Top	6 ϕ16 mm	5 ϕ16 mm
			Bottom	5 ϕ16 mm	4 ϕ16 mm
High-rise	0.45	0.60	Top	4 ϕ20 mm	3 ϕ20 mm
			Bottom	4 ϕ20 mm	3 ϕ20 mm

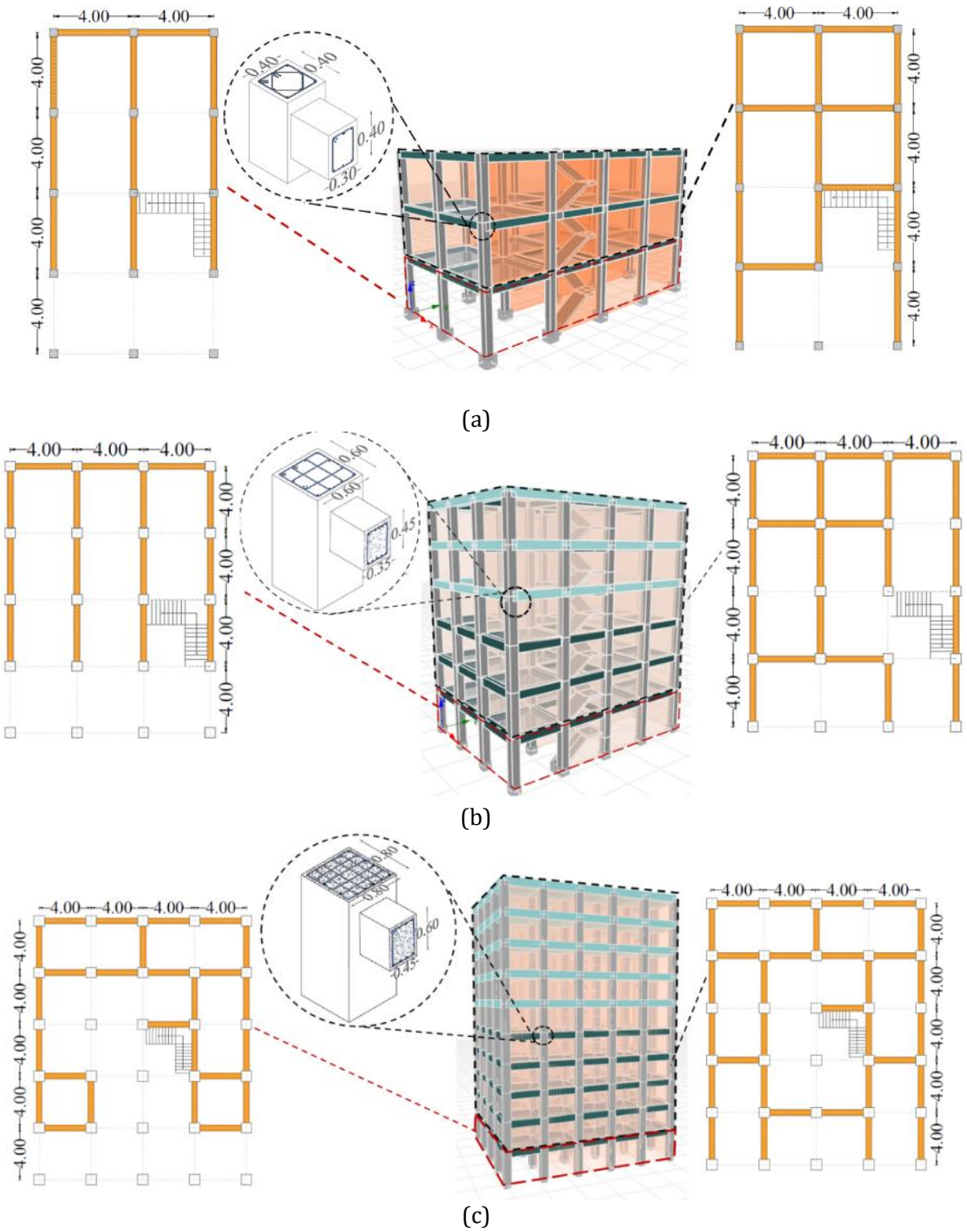

(a)

(b)

(c)

Fig. 1. Representative structural typologies adopted in the study: (a) low-rise building, (b) mid-rise building, and (c) high-rise building

A single beam reinforcement arrangement was adopted throughout the 3-story typology, whereas the 6- and 10-story typologies were divided into lower and upper story groups to represent the variation in reinforcement along the building height. A yield strength of 420 MPa was adopted for the reinforcing steel in all models, and transverse reinforcement in beams and columns consisted of 10 mm diameter stirrups spaced at 10 cm in the critical regions. The adopted story heights, vertical distribution of beam reinforcement groups, and reinforcement detailing of beams and columns are illustrated schematically in Fig. 2.

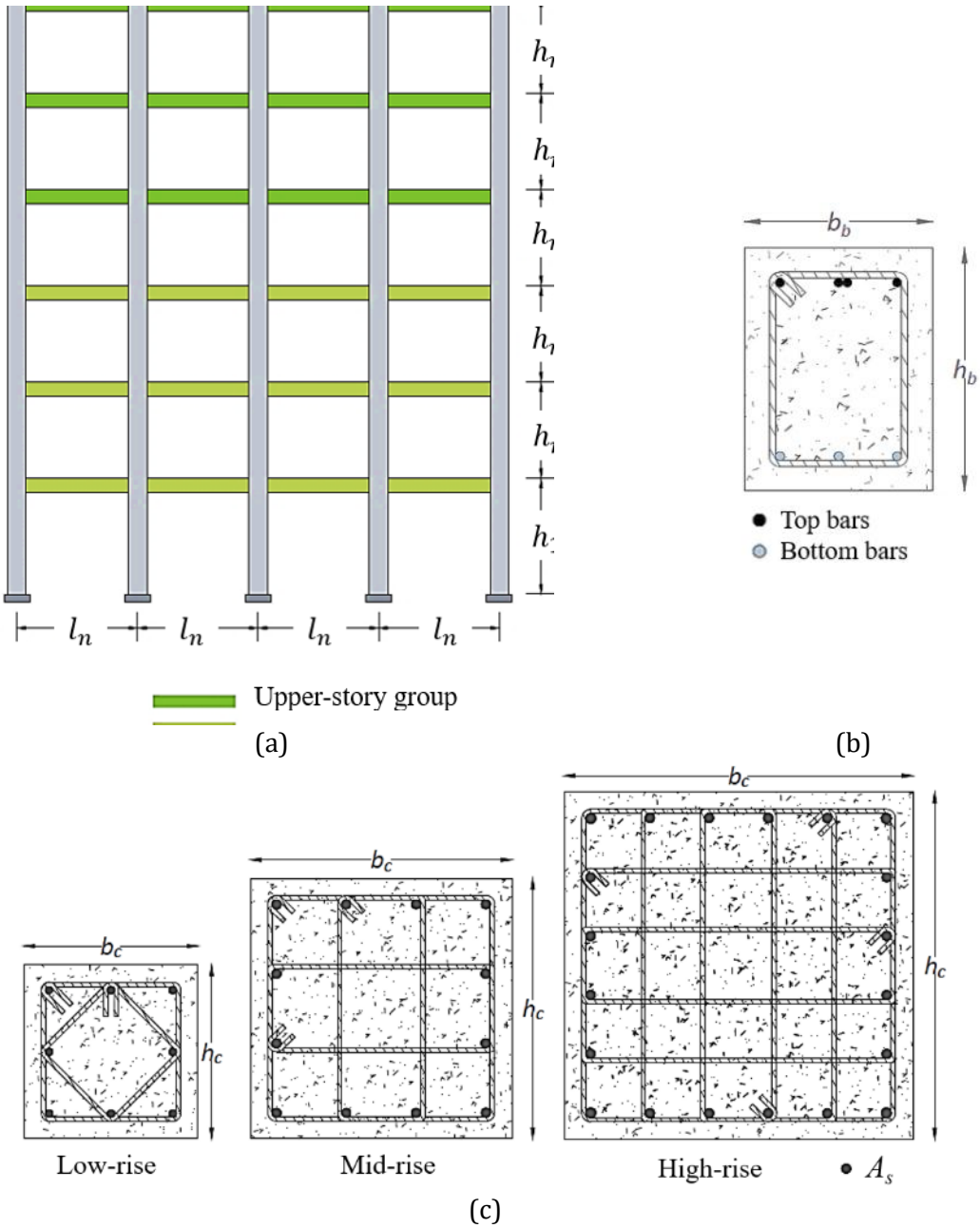

Fig. 2. Structural dimensions and reinforcement detailing adopted in the numerical models: (a) story heights and vertical distribution of beam reinforcement groups; (b) beam cross-section notation and longitudinal and transverse reinforcement; and (c) column cross-section notation and longitudinal reinforcement arrangements for the low-, mid-, and high-rise typologies

2.2 Structural Configurations and Numerical Modeling

For each typology, four structural configurations were evaluated, as shown in Fig. 3: frame (P), frame with staircases (P+S), frame with masonry infill walls (P+M), and frame with masonry infill walls and staircases (P+M+S). This comparison allowed the individual and combined effects of both components on lateral capacity, stiffness, ductility, and damage distribution to be identified.

Numerical modeling was performed in SeismoStruct. The reinforced concrete elements were represented using inelastic force-based beam-column elements with fiber sections. The constitutive model proposed by Mander et al. [20] was used for concrete, whereas the Menegotto and Pinto model [21] was adopted for reinforcing steel. Masonry infill walls were simulated using the nonlinear double-diagonal macromodel proposed by Crisafulli [22], which is widely used to represent the interaction between frames and infill panels [12,13].

To maintain consistency with the previously studied Portoviejo building typologies, the masonry input parameters were adopted from Ortega and Cagua [19]. The main properties considered were a panel thickness of t = 0.15 m, a masonry compressive strength of f_m = 1.469 MPa, and a diagonal-compression shear strength of f_{ws} = 0.44 MPa.

Staircases were explicitly incorporated into the structural model using inelastic force-based plastic-hinge frame elements (infrmFBPH), rather than shell elements or rigid plates. In this formulation, inelasticity is concentrated within prescribed plastic-hinge regions at the member ends, where the sectional response is evaluated through fiber integration, following the plastic-hinge integration approach proposed by Scott and Fenves [23]. The staircase elements were assigned the same concrete and reinforcing-steel constitutive models adopted for the reinforced-concrete frame members. Consequently, the nonlinear fiber-section formulation was also used to represent the inelastic response of the staircase members. When masonry infill walls or staircases were not explicitly modeled, their weight was included through equivalent loads to preserve the gravitational mass of the building and allow a consistent comparison among configurations.

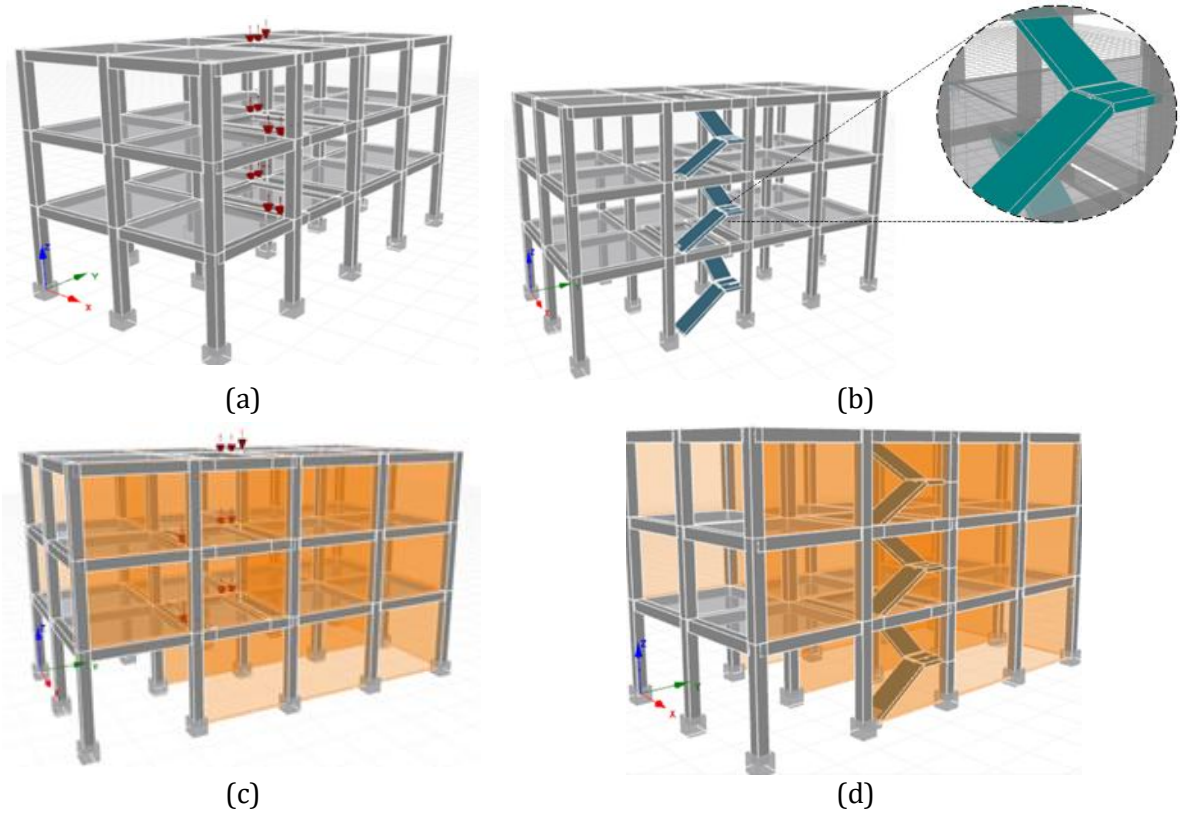

Fig. 3. Structural configurations analyzed: (a) P; (b) P+S; (c) P+M; (d) P+M+S

2.3 Seismic Demand

The seismic demand was defined for the city of Portoviejo according to NEC-SE-DS 2015, considering a high seismic hazard zone (VI), a zone factor Z = 0.50, an importance factor I = 1.0, and soil type D [5]. For the assessment, an elastic acceleration spectrum corresponding to a return period Tr of 475 years was used, together with a reference spectrum for Tr = 2475 years, obtained by scaling the design spectrum based on the site hazard curves, following the procedure applied by Ilbay (2025) [24]. Based on these spectra, the seismic demands associated with the three analyzed structural typologies were identified (Fig. 4). The seismic capacity of the buildings was evaluated through nonlinear static pushover analysis, applying an incremental lateral load pattern based on the first vibration mode. From the capacity curves, global parameters such as initial stiffness, base shear, ultimate displacement, ductility, and performance point were determined, following criteria commonly used in performance-based assessment [1-3].

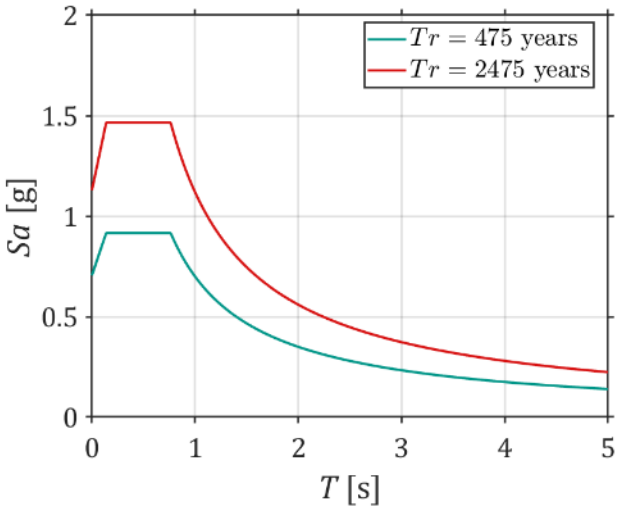

Fig. 4. Acceleration spectra considering soil type D, seismic zone VI, Z = 0.50, and I = 1.0, for Portoviejo

2.4 Performance and Damage Evaluation Criteria

The performance evaluation was carried out based on the performance point obtained for each typology and configuration, as well as on the global response parameters. In addition, the local damage distribution in the reinforced concrete elements and masonry infill panels were examined to identify differences in the response mechanisms according to building height and the presence of nonstructural elements. For the reinforced concrete elements, material strain limits associated with the behavior of concrete and steel were used, allowing damage in the main frame and in the structural elements of the staircase to be evaluated. The confined-concrete crushing limit of ε_c = 0.008 was adopted as a common damage-classification threshold for all typologies and was not calculated individually from the Mander model. This classification threshold is distinct from the confinement-dependent nonlinear concrete response represented by the constitutive model. For the masonry infill walls, dimensionless axial-strain thresholds of the equivalent compression strut were adopted to classify the equivalent damage states (Table 3). Together, these criteria made it possible to distinguish different damage levels in both the main lateral-load-resisting system and the infill panels, based on damage criteria reported in the literature.

Table 3. Criteria used for damage evaluation

Material	Legend	Description	Monitored quantity	Strain limit, ε (dimensionless)
Concrete		Unconfined concrete crushing	Concrete material strain	0.0035
		Confined concrete crushing		0.008
Steel		Steel yielding	Reinforcing-steel material strain	0.0025
		Steel fracture		0.1
Masonry		Slight damage	Equivalent-strut axial strain ε (-)	≤ 0.0015
		Moderate damage		0.0015 – 0.0030
		Extensive damage		0.0030 – 0.0060
		Complete damage		> 0.0060

Note: All strain limits are dimensionless. For concrete and reinforcing steel, the values correspond to material strains evaluated in the fiber sections. For masonry infill walls, the limits correspond to the axial strain of the equivalent compression strut and are distinct from interstory drift ratios. The confined-concrete limit of ε_c = 0.008 was adopted as a common damage-classification threshold for all typologies rather than being calculated individually from the Mander model.

3. Results and Discussion

Fig. 5 presents the capacity curves of the three analyzed typologies for the four structural configurations considered. In general terms, the inclusion of masonry infill walls and staircases modifies the global response, although their effect varies depending on the height of the structure. The seismic performance point was evaluated from the intersection between the structural capacity and the seismic demand corresponding to the design-level earthquake and the maximum considered earthquake, with return periods *Tr* of 475 and 2475 years, respectively. This allowed the variation in the structural response of each typology and configuration to be compared under different hazard levels.

Table 4 summarizes the main quantitative parameters derived from the capacity curves for all structural typologies and configurations. The values include the maximum base shear V_{max}, yield displacement Δ_y, performance-point displacement Δ_{pp}, and the corresponding displacement ductility demand μ_{pp} for *Tr* = 475 and 2475 years, together with the conservative interpretation limit Δ_{lim}. These parameters complement the graphical comparison presented in Fig. 5 and provide a direct basis for evaluating the influence of masonry infill walls and staircases on the global structural response.

In the low-rise building, the presence of masonry infill walls produced the greatest modification in the capacity curve, reflected in a marked increase in initial stiffness and lateral strength. As summarized in Table 4, V_{max} increased from 1104.1 kN for the bare frame (P) to 1247.6 and 1351.5 kN for P+M and P+M+S, corresponding to increases of approximately 13.0% and 22.4%, respectively. In parallel, Δ_y decreased from 0.040 m for P to 0.018 m for P+M and 0.022 m for P+M+S. This response was observed in both the P+M and P+M+S configurations, indicating that, in this type of building, masonry infills actively participate in the lateral behavior of the system. For *Tr* = 475 years, the corresponding displacement ductility demand, μ_{pp}, decreased from 2.46 for P to 1.87 for P+M and 1.51 for P+M+S, indicating a lower deformation demand relative to yielding in the infilled configurations at the design-level performance point. The exclusive incorporation of staircases (P+S) also produced an increase in stiffness with respect to the frame configuration (P), although to a lesser extent than that produced by the masonry infill walls.

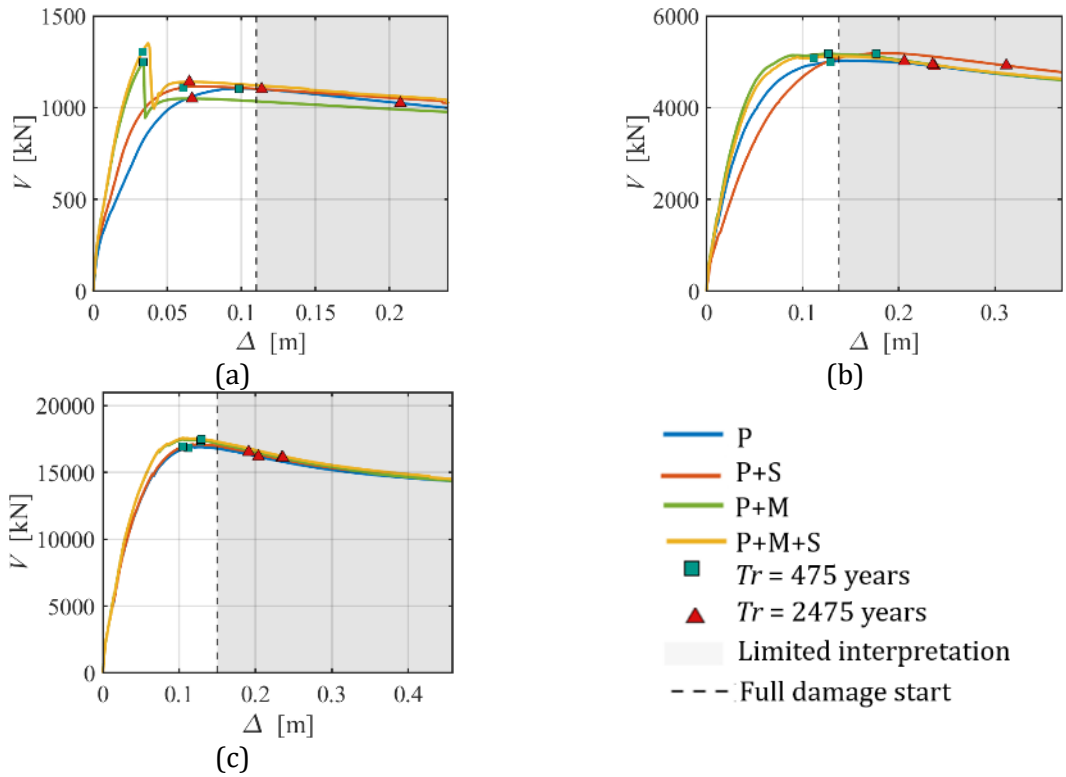

Fig. 5. Capacity curves in the X direction for the analyzed typologies: (a) low-rise building, (b) mid-rise building, and (c) high-rise building

In the mid-rise typology, the effect of masonry infill walls and staircases remained appreciable, although it was less pronounced than in the 3-story building. The configurations with masonry infill walls (P+M and P+M+S) exhibited steeper initial slopes and higher strength values than the frame model (P), but with more moderate differences. This behavior suggests that, as building height increases, the relative contribution of nonstructural elements to the global response decreases, although they still modify the lateral capacity and damage evolution. In the high-rise typology, the capacity curves of the different configurations showed smaller differences among them, indicating a lower global influence of masonry infill walls and staircases on the building response. In this case, the behavior was mainly governed by the flexibility of the resistance frame. However, although the global effect was smaller, this does not imply that the presence of these elements is irrelevant from a local perspective, since their influence may be reflected in the redistribution of internal forces and the concentration of damage in specific regions.

Table 4. Summary of capacity-curve parameters and performance-point demands

Typology	Config.	$V_{\max}$ (kN)	Δ_y (m)	$\Delta_{pp,475}$ (m)	$\mu_{pp,475}$	$\Delta_{pp,2475}$ (m)	$\mu_{pp,2475}$	$\Delta_{\lim}$ (m)
Low-rise	P	1104.116	0.040	0.098	2.46	0.207†	5.18†	0.110
	P+S	1115.749	0.028	0.061	2.17	0.114†	4.06†	0.110
	P+M	1247.556	0.018	0.034	1.87	0.067	3.70	0.110
	P+M+S	1351.509	0.022	0.033	1.51	0.065	2.95	0.110
Mid-rise	P	5024.919	0.051	0.129	2.53	0.237†	4.65†	0.138
	P+S	5185.819	0.076	0.177†	2.32†	0.312†	4.10†	0.138
	P+M	5175.364	0.043	0.127	2.95	0.235†	5.47†	0.138
	P+M+S	5120.986	0.046	0.112	2.43	0.206†	4.47†	0.138
High-rise	P	16909.013	0.051	0.112	2.20	0.204†	4.00†	0.150
	P+S	17104.651	0.055	0.105	1.91	0.191†	3.47†	0.150
	P+M	17477.018	0.050	0.128	2.56	0.234†	4.69†	0.150
	P+M+S	17577.855	0.052	0.129	2.48	0.236†	4.54†	0.150

Note: Δ_y denotes the yield displacement; Δ_{pp} denotes the roof displacement at the performance point; and $\mu_{pp} = \Delta_{pp}/\Delta_y$ denotes the displacement ductility demand at the corresponding performance point. Δ_{lim} denotes the conservative roof-displacement limit adopted to delimit the range of physical interpretation of the capacity curves and is not interpreted as an ultimate or collapse displacement. † Performance-point values beyond Δ_{lim} should be interpreted with caution.

Overall, masonry infill walls showed a more significant influence than staircases on initial stiffness and strength, especially in the low- and mid-rise typologies. Nevertheless, staircases also modify the structural response and should be considered in the numerical model. Although the capacity curves are presented up to the maximum displacement reached by the numerical procedure the response beyond the conservative global roof-displacement limits adopted for each typology should be interpreted with caution. In this study, the global collapse of the structure was not explicitly modeled; therefore, the final branch of the curve mainly reflects the numerical continuity of the analysis and does not necessarily represent a physically reliable structural capacity from a performance-based perspective. For this reason, conservative roof-displacement limits, denoted $\Delta_{\lim}$, were adopted to delimit the range of physical interpretation of the capacity curves. Values of 0.110, 0.138, and 0.150 m were adopted for the low-, mid-, and high-rise typologies, respectively, corresponding to global roof drift ratios of approximately 1.15%, 0.74%, and 0.49%. These limits do not represent ultimate or collapse displacements; beyond $\Delta_{\lim}$, the response is retained only as a numerical reference and should be interpreted with caution. This interpretation is consistent with Fig. 6, corresponding to the design-level earthquake (*Tr* = 475 years), where local damage is mainly concentrated in beams and columns of the lower stories, with a predominance of steel yielding and unconfined concrete crushing. Fig. 6 shows that, in the low-rise typology, the configurations with masonry infill walls reduce the overall extent of deformation, although critical zones remain at the base. In the mid-rise typology, the most marked concentration of damage is identified at the first level, whereas in the high-rise typology, damage is distributed over a larger portion of the height, with less pronounced differences among configurations.

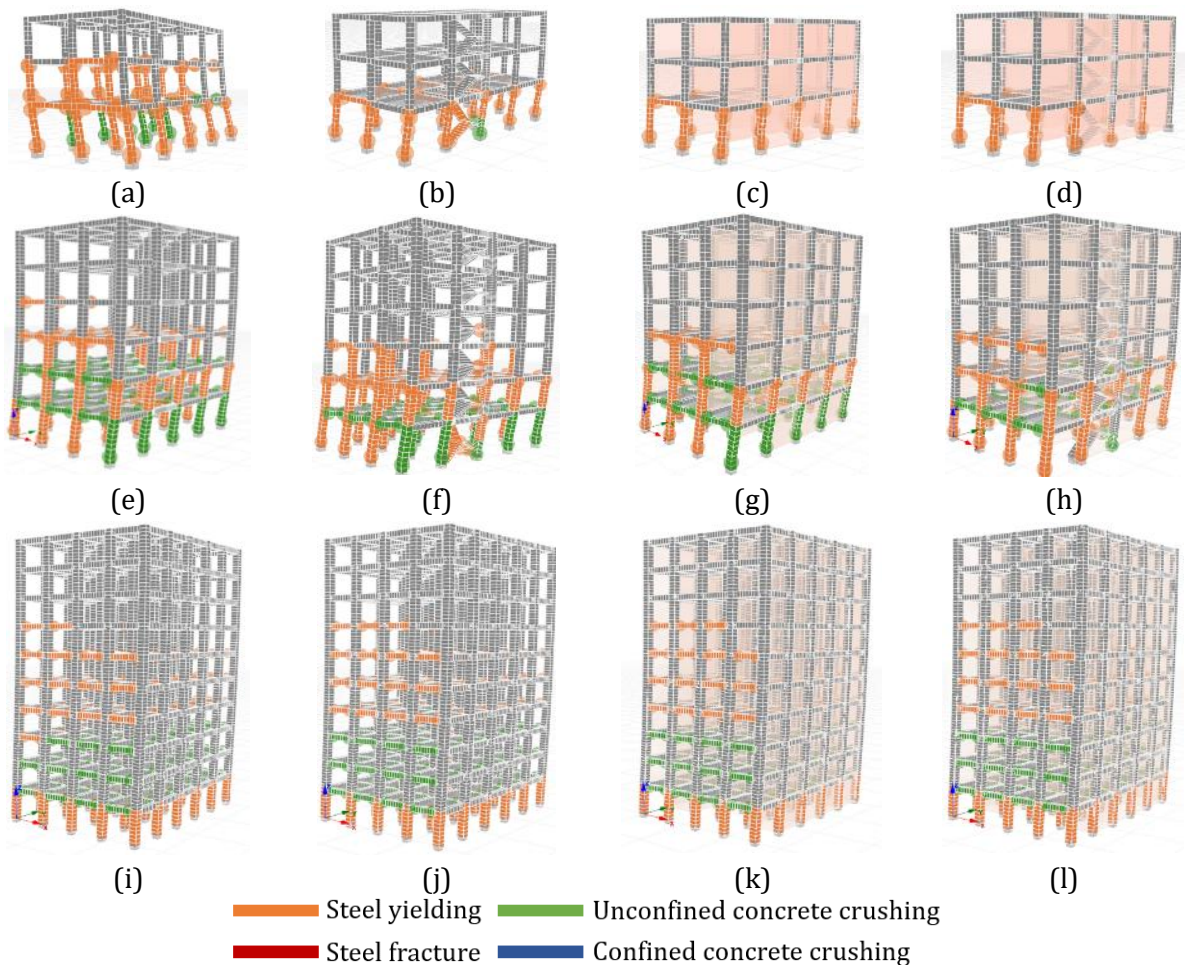

Fig. 6. Local damage distribution in beams and columns (*Tr* = 475 years and pushover analysis in the X direction). Low-rise typology: (a) P, (b) P+S, (c) P+M, and (d) P+M+S. Mid-rise typology: (e) P, (f) P+S, (g) P+M, and (h) P+M+S. High-rise typology: (i) P, (j) P+S, (k) P+M, and (l) P+M+S

Fig. 7 shows the spatial distribution of local damage in reinforced concrete structural elements for the extreme demand scenario (*Tr* = 2475 years). Compared with the design-level earthquake, an increase is observed in both the extent and severity of damage, particularly in the mid- and high-rise typologies, where damage states associated with confined concrete crushing appear more clearly in the lower stories. In the low-rise typology, although damage continues to be mainly concentrated at the first level, the configurations with masonry infill walls maintain a lower overall dispersion of deformation compared with the bare frame. In the mid-rise typology, damage accumulation in columns and beams at the first level becomes more severe, indicating a pronounced concentration of seismic demand. This response is further examined through the interstory drift profiles presented in Fig. 8. In the high-rise typology, the global differences among configurations remain more moderate; however, the increase in damage in the lower half of the building shows that, even when the global influence of masonry infills and staircases decreases with height, their local effects remain relevant. To complement the local damage distributions, Fig. 8 presents the interstory drift ratio (IDR) profiles along the building height for the four structural configurations and both seismic demand levels. The results show a clear concentration of deformation demand in the lower stories of the low- and mid-rise typologies. In the mid-rise building, the largest IDRs occur within the first two stories and decrease markedly toward the upper levels, particularly for *Tr* = 2475 years. This response is consistent with the concentration of beam and column damage observed in Fig. 6 and Fig. 7 and supports the identified tendency toward soft-story-type behavior. In contrast, the high-rise typology exhibits a more distributed drift profile over the building height, although the largest demand remains concentrated in its lower portion.

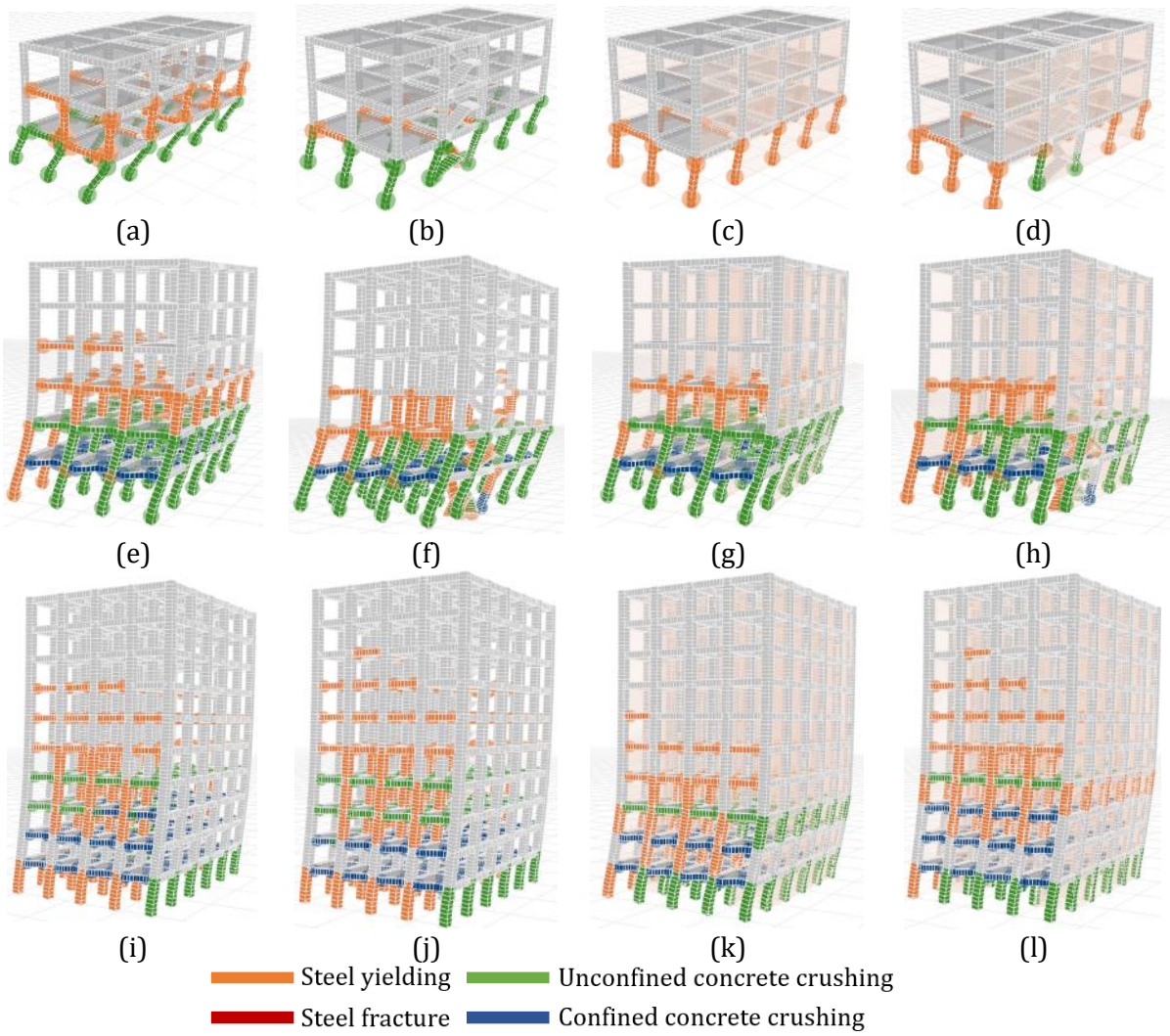

Fig. 7. Local damage distribution in beams and columns (*Tr* = 2475 years and pushover analysis in the X direction). Low-rise typology: (a) P, (b) P+S, (c) P+M, and (d) P+M+S. Mid-rise typology: (e) P, (f) P+S, (g) P+M, and (h) P+M+S. High-rise typology: (i) P, (j) P+S, (k) P+M, and (l) P+M+S

These IDR profiles therefore provide a quantitative counterpart to the spatial damage patterns and clarify the height-dependent distribution of seismic deformation demand. Fig. 9 shows that damage in the masonry infill walls is mainly concentrated in the lower stories, where the largest interstory deformations also develop. When moving from the design-level earthquake (*Tr* = 475 years) to the extreme earthquake (*Tr* = 2475 years), both the extent and severity of damage increase, with a transition from predominantly slight and moderate damage states toward a greater presence of extensive and complete damage. This pattern is consistent with the vertical stiffness irregularity of the analyzed typologies, which are characterized by a more flexible ground story and greater continuity of panels in the upper stories. This interpretation is also supported by the IDR profiles in Fig. 8, which show lower interstory deformation demands in the upper stories than in the lower portion of the low- and mid-rise buildings. This analytical response is consistent with post-earthquake observations reported for Portoviejo after the 2016 Ecuador earthquake, where reinforced-concrete buildings with taller and more open ground floors associated with commercial use, together with a reduced presence of masonry infill walls at the first level, exhibited increased vulnerability to deformation and damage concentration in the lower stories [7]. The damage distribution shown in Fig. 9 indicates that, in the low-rise typology, masonry infill walls contribute significantly to global stiffness, limiting the overall deformation of the building; however, the most severe damage is concentrated in the panels at the first level. For *Tr* = 475 years, slight and moderate damage predominates in the upper stories, whereas extensive and complete damage appears at the base; for *Tr* = 2475 years, this concentration intensifies.

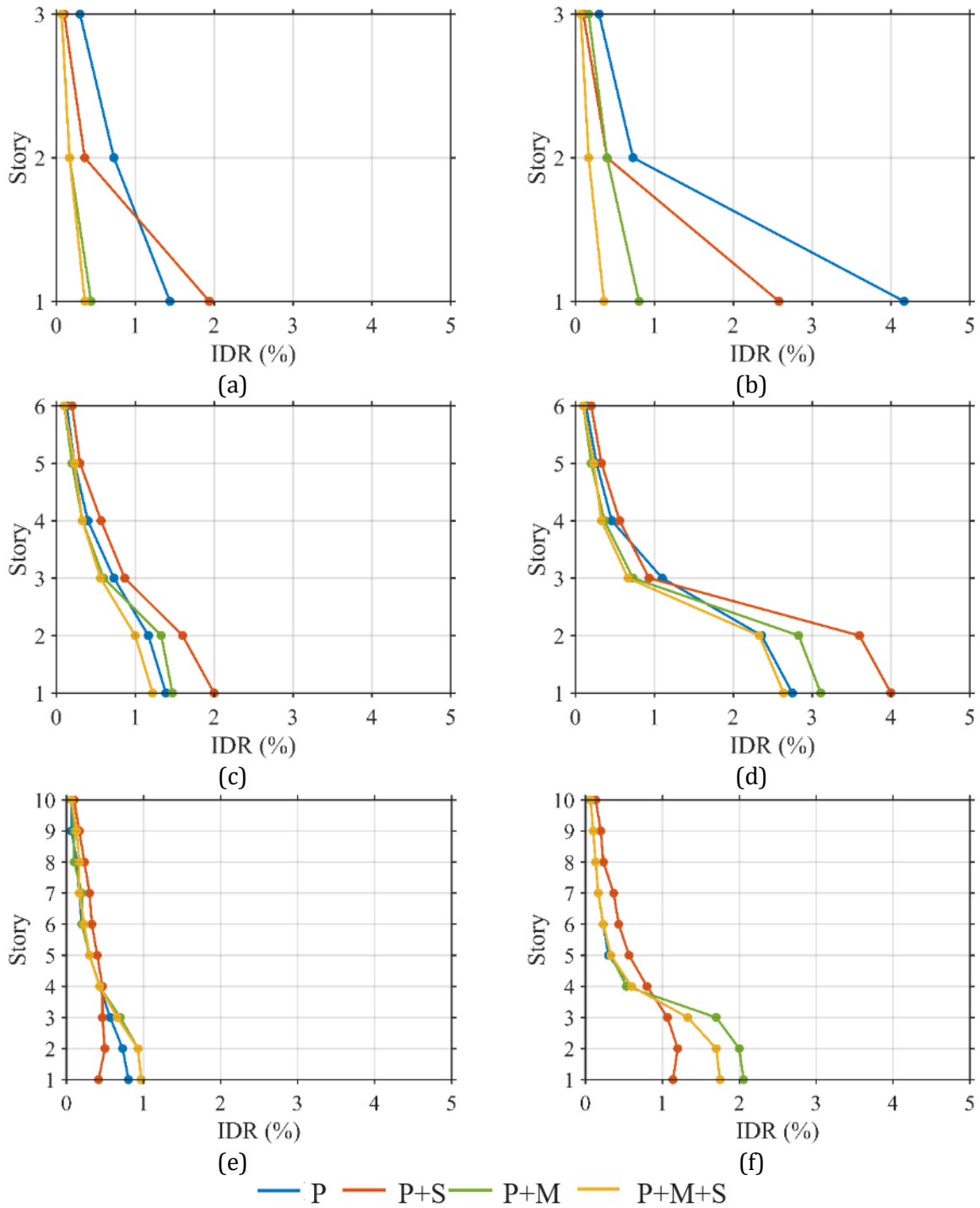

Fig. 8. IDR profiles in the X direction for the four structural configurations under the design-level and maximum-considered seismic demands: low-rise building at (a) *Tr* = 475 years and (b) *Tr* = 2475 years; mid-rise building at (c) *Tr* = 475 years and (d) *Tr* = 2475 years; and high-rise building at (e) *Tr* = 475 years and (f) *Tr* = 2475 years

In the mid-rise typology, the most critical response is observed: even for *Tr* = 475 years, a continuous band of severe damage appears in the lower stories, which extends and becomes more severe for *Tr* = 2475 years, confirming the pronounced concentration of deformation demand in the lower stories and supporting the identified soft-story-type response. In the high-rise typology, the relative contribution of masonry infill walls to global behavior is lower, but their local effect remains relevant, since damage is concentrated in the lower part of the building and becomes more continuous under the extreme demand. To complement the spatial damage distribution, Fig. 10 quantifies the masonry response as the percentage of infill panels reaching or exceeding each damage-state axial-strain threshold.

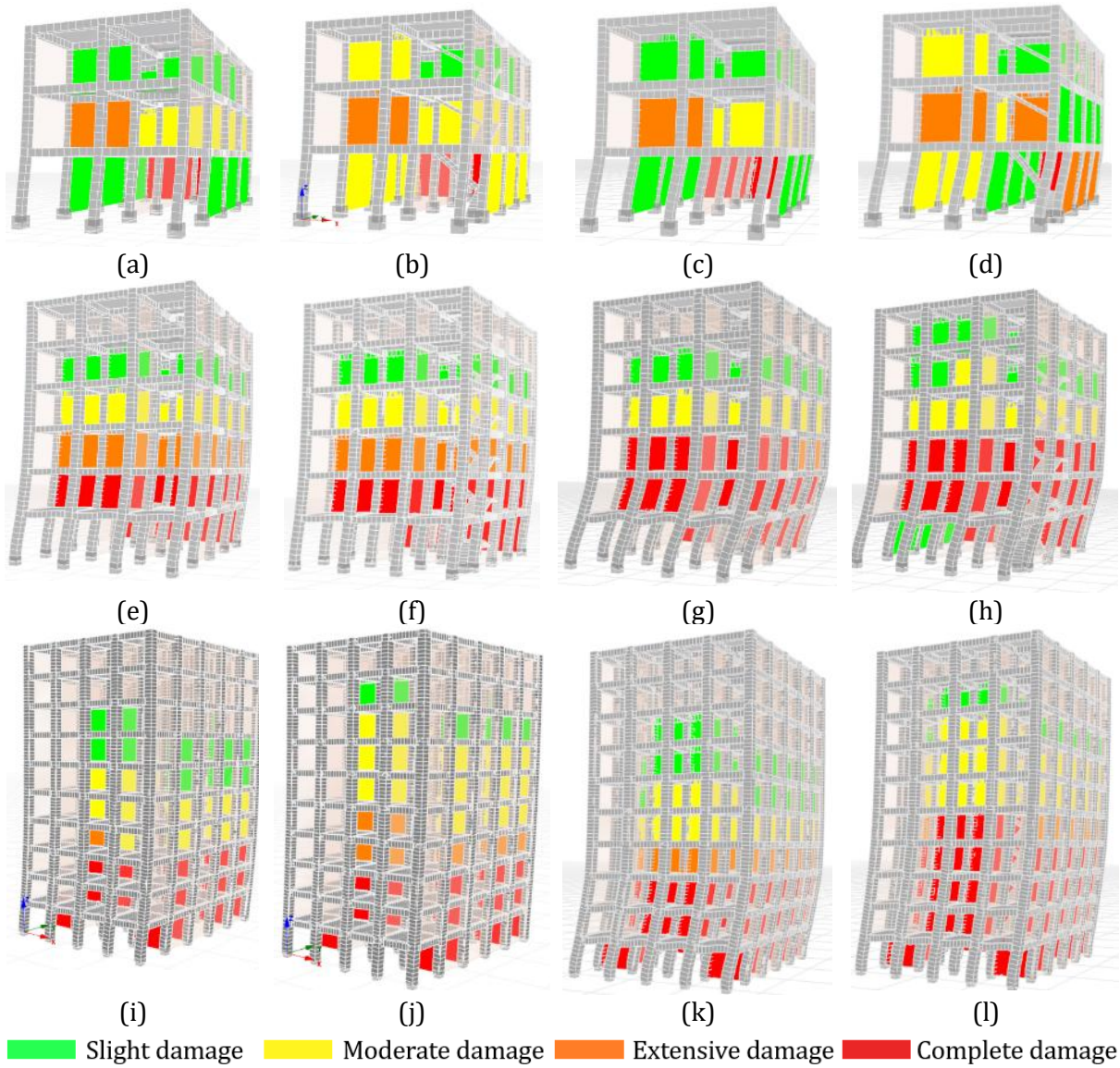

Fig. 9. Damage localization and severity in masonry infill walls. Low-rise typology: (a) P+M and (b) P+M+S for *Tr* = 475 years; (c) P+M and (d) P+M+S for *Tr* = 2475 years. Mid-rise typology: (e) P+M and (f) P+M+S for *Tr* = 475 years; (g) P+M and (h) P+M+S for *Tr* = 2475 years. High-rise typology: (i) P+M and (j) P+M+S for *Tr* = 475 years; (k) P+M and (l) P+M+S for *Tr* = 2475 years

The percentages were calculated with respect to the total number of infill panels in each typology: 39 panels for the low-rise building, 120 for the mid-rise building, and 314 for the high-rise building. The comparison was performed for both *Tr* = 475 and 2475 years. The results provide a quantitative counterpart to Fig. 9 and show how the proportion of panels reaching progressively more severe damage thresholds changes with building height, structural configuration, and seismic demand.

The comparison among configurations indicates that the incorporation of staircases does not eliminate the concentration of damage at the base, although it modifies its spatial distribution, in some cases making it more dispersed or increasing the proportion of panels with moderate and extensive damage. In the P+S and P+M+S configurations, the staircase–frame interaction modifies the local response of the members adjacent to the intermediate landings. The staircase flights and landings restrain the deformation of the connected column segments, effectively reducing their deformable length and promoting a localized concentration of demand. This behavior is consistent with a short-column-type response, expressed in the present models through changes in the local damage distribution around the staircase region. Accordingly, the influence of the staircase is interpreted primarily as a local response mechanism rather than as a dominant contributor to the global capacity of the building.

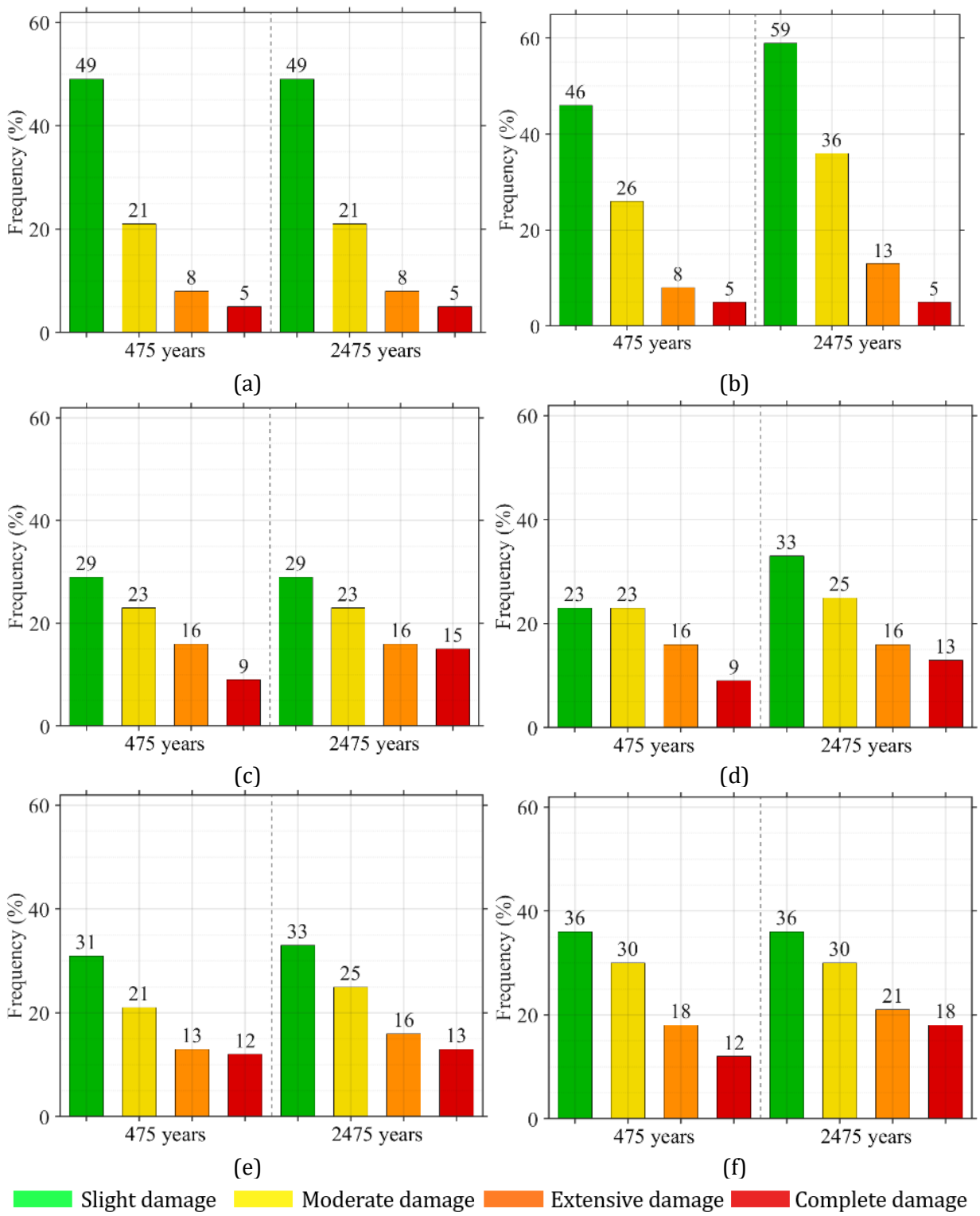

Fig. 10. Percentage of masonry infill panels reaching or exceeding each damage-state axial-strain threshold for *Tr* = 475 and 2475 years: (a) low-rise P+M; (b) low-rise P+M+S; (c) mid-rise P+M; (d) mid-rise P+M+S; (e) high-rise P+M; and (f) high-rise P+M+S. Percentages are referred to the total number of infill panels in each typology (39, 120, and 314 panels for the low-, mid-, and high-rise buildings, respectively).

4. Conclusions

The inclusion of masonry infill walls and staircases significantly modified the seismic response of the analyzed buildings, although their influence depended on building height. The results indicate that masonry infill walls constitute a non-negligible component in the seismic performance

assessment of the analyzed buildings, particularly because their contribution modifies the initial stiffness and lateral strength of the system. Their influence is more pronounced than that of the staircases at the global response level, whereas staircases, despite their smaller global contribution, remain relevant to the local damage distribution and frame response.

In the low-rise typology, masonry infill walls produced the greatest increase in stiffness and strength, reducing the demanded global displacements and improving the structural performance under the design-level earthquake. Quantitatively, the maximum base shear increased by approximately 13.0% for P+M and 22.4% for P+M+S relative to the bare-frame configuration. However, this benefit was accompanied by a reduction in deformation capacity and by the persistence of critical damage zones at the first level, indicating that the reduced global deformation demand does not necessarily imply lower local vulnerability, since the stiffness discontinuity and infill–frame interaction may concentrate force demands, including shear, in the ground-floor columns.

The mid-rise typology exhibited the most critical behavior with respect to the interaction between the frame, masonry infill walls, and staircases. The concentration of beam and column damage in the lower stories, together with the IDR profiles showing the largest deformation demands within the first two stories, identifies the mid-rise typology as the most susceptible among the analyzed cases to the development of a lower-story deformation mechanism under the adopted seismic demands. This response is associated with the vertical stiffness irregularity of the building and is consistent with soft-story-type behavior.

In the high-rise typology, the global differences among configurations were smaller, indicating that the response was mainly governed by the flexibility of the resisting frame. Nevertheless, under high levels of seismic demand, local effects on the damage distribution persisted, especially in the lower half of the building, confirming that the influence of masonry infilling walls and staircases does not completely disappear with height. In particular, the staircase–frame interaction locally modifies the stiffness distribution and seismic load path, leading to redistribution of force and deformation demands even when its influence on the global capacity is comparatively limited.

Overall, the results show that omitting masonry infill walls and staircases may lead to an unrealistic representation of the seismic behavior of typical building stock in Portoviejo, especially in low- and mid-rise structures. Therefore, for seismic safety assessments of existing mid-rise RC buildings in Portoviejo with architectural and structural characteristics similar to those analyzed herein, the explicit consideration of masonry infill walls and staircases in the numerical model is recommended within the NEC-SE-DS assessment framework, particularly when evaluating lower-story deformation and damage concentration.

The findings are limited to the three representative typologies, structural configurations, and nonlinear static analysis framework considered in this study. Future research may extend this assessment through nonlinear dynamic analyses and a broader range of building geometries and infill/staircase configurations to evaluate the generality of the observed response trends.

References

[1] Applied Technology Council. Seismic evaluation and retrofit of concrete buildings, ATC-40. Redwood City, CA: Applied Technology Council; 1996.

[2] Federal Emergency Management Agency. Improvement of nonlinear static seismic analysis procedures, FEMA 440. Washington, DC: Federal Emergency Management Agency; 2005.

[3] Zameeruddin M, Sangle KK. Performance-based seismic assessment of reinforced concrete moment resisting frame. Journal of King Saud University - Engineering Sciences. 2021;33(3):153-165. https://doi.org/10.1016/j.jksues.2020.04.005

[4] Beauval C, Marinière J, Yepes H, Audin L, Nocquet JM, Alvarado A, et al. A new seismic hazard model for Ecuador. Bulletin of the Seismological Society of America. 2018;108(3A):1443-1464. https://doi.org/10.1785/0120170259

[5] MIDUVI. NEC-SE-DS: Norma Ecuatoriana de la Construcción - Seguridad Estructural - Diseño Sismo Resistente. Quito, Ecuador: Ministerio de Desarrollo Urbano y Vivienda; 2014.

[6] Aguiar R, Cagua B. Métodos simplificados para el análisis y la evaluación rápida de estructuras. 1st ed. Guayaquil, Ecuador: Lidinci S.A.; 2023.

[7] Aguiar R, Mieles Y. Análisis de los edificios que colapsaron en Portoviejo durante el terremoto del 16 de abril de 2016. Revista Internacional de Ingeniería de Estructuras. 2016;21(3):257-282.
[8] Kagermanov A, Ceresa P, Morales E, Poveda J, O'Connor J. Seismic performance of RC buildings during the Mw 7.8 Muisne (Ecuador) earthquake on April 2016: field observations and case study. Bulletin of Earthquake Engineering. 2017;15(12):5167-5189. https://doi.org/10.1007/s10518-017-0182-y
[9] Barros L. Nonlinear analysis of a reinforced concrete building with masonry infill affected by the April 16, 2016 earthquake in Ecuador [Master's thesis]. Santiago, Chile: Pontificia Universidad Católica de Chile; 2020.
[10] Vielma JC, Aguiar R, Frau C, Zambrano A. Irregularity of the distribution of masonry infill panels and its effect on the seismic collapse of reinforced concrete buildings. Applied Sciences. 2021;11(18):8691. https://doi.org/10.3390/app11188691
[11] Cagua-Gómez BJ, Aguiar-Falconí RR, Pilatasig-Caizaguano JE. Influencia de la mampostería de relleno en el desempeño sísmico de estructuras aporticadas de hormigón armado. Ingeniare. Revista Chilena de Ingeniería. 2022;30(3):513-527. https://doi.org/10.4067/S0718-33052022000300513
[12] De Angelis A, Pecce MR. The role of infill walls in the dynamic behavior and seismic upgrade of a reinforced concrete framed building. Frontiers in Built Environment. 2020;6:590114. https://doi.org/10.3389/fbuil.2020.590114
[13] Falcão Moreira R, Varum H, Castro JM. Influence of masonry infill walls on the seismic assessment of non-seismically designed RC framed structures. Buildings. 2023;13(5):1148. https://doi.org/10.3390/buildings13051148
[14] Zhang X, Zhou Y, Liu X, Zheng Y, Qi Z. Study on seismic performance of RC frame structures considering the effect of infilled walls. Buildings. 2024;14(7):1907. https://doi.org/10.3390/buildings14071907
[15] Ahmed OH, Hazem AR, Shawky AA. Seismic performance of staircases in the 3D analysis of RC building. Civil Engineering Journal. 2022;7:114-123. https://doi.org/10.28991/CEJ-SP2021-07-08
[16] Jiang HJ, Gao HY, Wang B. Seismic damage analyses of staircases in RC frame structures. Advanced Materials Research. 2012;446-449:2326-2330. https://doi.org/10.4028/www.scientific.net/AMR.446-449.2326
[17] Karaaslan A, Avşar Ö. Seismic response of substandard RC frame buildings in consideration of staircases. Earthquakes and Structures. 2019;17(3):283-295.
[18] Türer A. Seismic performance of RC staircases in the 2023 Kahramanmaraş earthquakes: field observation, damage patterns and evacuation risk. Bulletin of Earthquake Engineering. 2026;24(4):2135-2159. https://doi.org/10.1007/s10518-025-02359-8
[19] Ortega D, Cagua BJ. Influence of masonry walls and stairs on the seismic behavior of reinforced concrete buildings: a case study in Portoviejo. International Review of Civil Engineering (IRECE). 2025;16(2):91-103. https://doi.org/10.15866/irece.v16i2.25024
[20] Mander JB, Priestley MJN, Park R. Theoretical stress-strain model for confined concrete. Journal of Structural Engineering. 1988;114(8):1804-1826. https://doi.org/10.1061/(ASCE)0733-9445(1988)114:8(1804)
[21] Menegotto M, Pinto PE. Method of analysis for cyclically loaded reinforced concrete plane frames including changes in geometry and non-elastic behavior of elements under combined normal force and bending. In: IABSE Symposium on Resistance and Ultimate Deformability of Structures Acted on by Well-Defined Repeated Loads; 1973; Lisbon, Portugal. p. 15-22.
[22] Crisafulli FJ. Seismic behaviour of reinforced concrete structures with masonry infills [PhD Thesis]. Christchurch, New Zealand: University of Canterbury; 1997.
[23] Scott MH, Fenves GL. Plastic hinge integration methods for force-based beam-column elements. Journal of Structural Engineering. 2006;132(2):244-252. https://doi.org/10.1061/(ASCE)0733-9445(2006)132:2(244)
[24] Ilbay D. Análisis de fragilidad sísmica de edificaciones de hormigón armado con columnas cortas [Master's thesis]. Quito, Ecuador: Universidad Central del Ecuador; 2025.